Journal of Materials Chemistry C

PAPER

View Article Online
View Journal | View Issue



Cite this: J. Mater. Chem. C, 2014, 2, 3407

# Stabilizing cations in the backbones of conjugated polymers†

Thomas P. Voortman,[ab] Hilde D. de Gier,[b] Remco W. A. Havenith[bc] and Ryan C. Chiechi*[ab]

Received 8th November 2013
Accepted 14th January 2014

DOI: 10.1039/c3tc32204a

www.rsc.org/MaterialsC

We synthesized a cross-conjugated polymer containing ketones in the backbone and converted it to a linearly conjugated, cationic polyarylmethine *via* a process we call "spinless doping" to create a new class of materials, conjugated polyions. This process involves activating the ketones with a Lewis acid and converting them to trivalent cations *via* the nucleophilic addition of electron-rich aryl moieties. Spinless doping lowers the optical band gap from 3.26 to 1.55 eV while leaving the intrinsic semiconductor properties of the polymer intact. Electrochemical reduction (traditional doping) further decreases the predicted gap to 1.18 eV and introduces radicals to form positive polarons; here, n-doping produces a p-doped polymer in its metallic state. Treatment with a nucleophile (NaOMe) converts the cationic polymer to a neutral, non-conjugated state, allowing the band gap to be tuned chemically, post-polymerization. The synthesis of these materials is carried out entirely without the use of Sn or Pd and relies on scalable Friedel–Crafts chemistry.

## 1 Introduction

The utility of conjugated polymers as electro-optical materials is their unique combination of semiconducting and mechanical properties; they can be processed from solution into devices with similar functionality to their more brittle inorganic counterparts. Devices like field-effect transistors and organic photovoltaics utilize conjugated polymers in their undoped, semiconducting state,[1] while sensors and other devices utilize their doped, metallic state(s).[2] Virtually all conjugated polymers can be converted from neutral intrinsic semiconductors to charged, metallic states by the addition (n-doping) or removal (p-doping) of electrons. These are redox processes that create the radical anions/cations (polarons) that serve as charge-carriers and that impart the dramatic increase in conductivity that is associated with doping. This process also introduces unpaired spins that create mid-gap states, significantly reducing the band-gap, and red-shifting the optical absorption (*i.e.*, the optical properties are mainly affected by the creation of new states rather than the energies of the bands being shifted by the presence of charges). One exception is poly(aniline) (PANI), which can be converted to its metallic state(s) by protonation; however, this process too is the result of the spontaneous formation of unpaired spins.[3] We previously reported an n-dopable conjugated polymer in which the influence of spin and charge could be separated.[4] This polymer was based on a cross-conjugated polyketone that could be reduced (n-doped) into two distinct states, a normal, metallic, doped state and a charged, but semiconducting state. These states exhibited clear spectroscopic differences and differences in conductivity, however, they were transient, existing only while held at cathodic potentials under air-free conditions.

This paper describes the stabilization of permanent charges *via* "spinless doping," a process in which a cross-conjugated polyketone is converted to a linearly conjugated polymer that is a charged, intrinsic semiconductor by the addition of nucleophiles during post-polymerization modification. Unlike the previous polyketones, which were doped only transiently, these conjugated polyions (CPIs) are robust, air-stable, and exhibit dynamic band gaps. They separate the influences of the unpaired electrons that result from traditional redox doping from the inclusion of charges and show dramatic physical changes, including solubility, yet the position of the conduction band (determined electrochemically) remains almost unchanged from their cross-conjugated precursors. Although the polymers presented in this paper represent a proof-of-concept and have not yet been optimized for device applications, they are low band gap (~1.5 eV) intrinsic semiconductors that are synthesized entirely without Pd or Sn (Scheme 1). The monomers are prepared by nucleophilic displacement and the polymers by the same Friedel–Crafts polycondensation that was initially used to prepare poly(ether ketone), an engineering

[a]Stratingh Institute for Chemistry, University of Groningen, Nijenborgh 4, 9747 AG Groningen, the Netherlands. E-mail: r.c.chiechi@rug.nl

[b]Zernike Institute for Advanced Materials, University of Groningen, Nijenborgh 4, 9747 AG Groningen, the Netherlands

[c]Ghent Quantum Chemistry Group, Department of Inorganic and Physical Chemistry, Ghent University, Krijgslaan 281, B-9000 Gent, Belgium

† Electronic supplementary information (ESI) available. See DOI: 10.1039/c3tc32204a

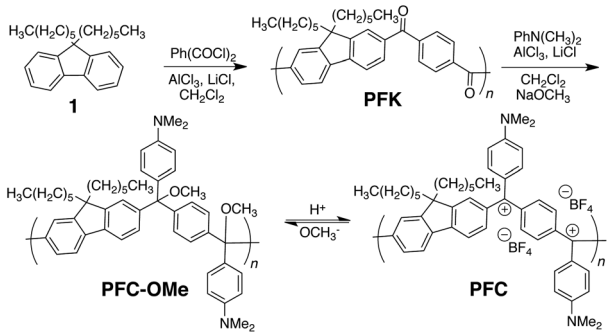


Scheme 1

plastic, on a pilot scale.[5–7] (It was later replaced with a process allowing for better, higher-boiling solvents.[8]) Spinless doping is accomplished with Lewis acid activation and treatment with *N*,*N*-dimethylaniline. Thus, CPIs are built on scalable chemistry, which is an important feature of a conjugated polymer in the context of technological applications as an optoelectronic material;[9,10] the lack of a scalable, industrially relevant synthetic route precludes commercial/technological applications.

Structurally, the CPIs presented in this paper are polyarylmethines (PAMs); however, PAMs are traditional conjugated polymers that must be redox doped and are, therefore, not related to CPIs beyond structural similarities.[11–16] Electronically, CPIs resemble conjugated polymers with trivalent atoms in the backbone such as boron[17–21] or nitrogen.[22] In fact, CPIs are isoelectronic with boron-containing polymers in that the carbocations possess an empty p-orbital, but they are charged because of the position of carbon in the periodic table. Nitrogen-containing polymers possess a full p-orbital, which means that they can potentially undergo spinless doping by protonation, however, the protonation of a full p-orbital will create an $sp^3$ hybridized nitrogen, disrupting the conjugated backbone. There are also cation-containing polymers with imidizolium units in the backbone, however, these charges do not reside in the conjugation pathway of the backbone.[23,24] Thus, while CPIs are structurally and electronically similar to PAMs and boron/nitrogen-containing polymers, they combine the properties of these different polymers in a unique way to form a new class of conjugated polymers with dynamically tunable band-gaps in the semi-conducting state (*i.e.*, the conjugation length can be controlled post-synthetically and without redox) due to the presence of stable cations in the conjugated backbone.

# 2 Experimental

## 2.1 General

All reagents and solvents were purchased from commercial sources and used without further purification unless otherwise indicated. NMR spectra were measured using a Varian AMX400 (400 MHz) instrument at 25 °C. FT-IR spectra were recorded on a Nicolet Nexus FT-IR fitted with a Thermo Scientific Smart iTR sampler. GPC measurements were done on a Spectra Physics AS 1000 series machine equipped with a Viskotek H-502 viscometer and a Shodex RI-71 refractive index detector. The columns (PLGel 5m mixed-C) (Polymer Laboratories) were calibrated using narrow disperse polystyrene standards (Polymer Laboratories). Samples were made in THF or $CHCl_3$ at a concentration of ~2.5 mg $mL^{-1}$. UV/Vis measurements were carried out on a Jenway 6715 spectrometer in 1 cm fused quartz cuvettes with concentrations of 0.03–0.1 mg $mL^{-1}$ in $CH_2Cl_2$. **PFK** and **PFC** were also measured in an acidic environment by dissolving a few drops of $H_2SO_4$ in $CH_2Cl_2$. EPR spectra were recorded on a Magnettech MiniScope MS400 using a quartz capillary at a concentration of 0.5–1 mM in THF and dichloroethane.

## 2.2 Monomer

**9,9-Dihexyl-9H-fluorene (1).**[25] Fluorene (2.5 g; 15.04 mmol) was dissolved in 150 mL THF in a dried three-necked round-bottom flask. The solution was then cooled to −78 °C with stirring and 22.6 mL of *n*-BuLi in hexane (1.6 M) rendering the solution orange. After stirring for 2 h, 1-bromohexane (6.2 g; 37.6 mmol) in 25 mL THF was added dropwise over 15–20 min. after which the solution was allowed to warm up to rt and stirring was continued for 24 h. The reaction mixture was quenched by pouring it over ice $H_2O$ before extracting with ether (2 × 150 mL). The combined organic layers were washed with DI $H_2O$, brine, dried over $Na_2SO_4$ and the solvent was removed by rotary evaporation, to yield the crude produce as a pale yellow oil. The produce was then dissolved in a small amount of ether and purified by column chromatography on silica gel and *n*-heptane as the eluent, before being dried *in vacuo* for 24 h at 200 mTorr to afford **1** as a colorless/white semi-solid (4.04 g; 80% yield). $^1$H NMR (400 MHz, $CDCl_3$) $\delta$ 7.70 (d, $J$ = 6.2 Hz, 2H), 7.36–7.27 (m, 6H), 1.99–1.92 (m, 4H), 1.15–1.00 (m, 12H), 0.76 (t, $J$ = 7.1 Hz, 6H), 0.66–0.55 (m, $J$ = 11.3 Hz, 4H). FT-IR (ATR) 3064, 3039, 3013, 2954, 2925, 2855, 1940, 1902, 1866, 1794, 603, 1583, 1476, 1447, 1377, 1340, 1287, 1217, 1154, 1127, 1104, 1030, 1005, 932, 890, 863, 771, 733, 636, 620 $cm^{-1}$.

## 2.3 Polymers

**Poly[(9,9-dihexylflourene)-*alt*-(1,4-phenylene)dimethanone] (PFK).** $AlCl_3$ (6.004 g; 45.024 mmol) and LiCl (10 wt% of $AlCl_3$) were added to 200 mL of freshly distilled $CH_2Cl_2$ in a dried three-necked round-bottom flask. To a second dried flask was added **1** (5.021 g; 15.008 mmol) and terephthaloyl chloride (3.047 g; 15.008 mmol), to 100 mL dry $CH_2Cl_2$. The Lewis acid solution was cooled to 0 °C and the monomer solution was slowly added by cannula, under vigorous stirring, resulting in a deep red slurry and the reaction mixture was then refluxed for 72 h under argon. Cooled down to rt the reaction mixture was quenched by pouring it out over stirring 1 N HCl/ice in an Erlenmeyer flask before extracting with $CH_2Cl_2$ (200 mL). The organic layer was washed with aqueous NaOH and HCl solutions and finally with brine. Any insolubles were removed by filtration. The organic phase was concentrated to dryness, redissolved in a minimal amount of hot THF and precipitated into a large excess of ice-cold $CH_3OH$ (1000 mL) and the precipitate was concentrated by centrifugation at 4000 rpm for

 

20 min and filtered over a soxhlet timble. The produce was purified further *via* continuous soxhlet extraction with $CH_3OH$, $CH_3COCH_3$, and $CHCl_3$ to afford **PFK** from the $CHCl_3$ fraction, after removal of the solvent by rotary evaporation, as a yellow powder (2.76 g; 40%). $^1$H NMR (400 MHz, $CDCl_3$) $\delta$ 8.37–7.27 (m, 10H), 2.28–1.74 (m, 4H), 1.36–0.81 (m, 12H), 0.86–0.39 (m, 10H). FT-IR (ATR) 3054, 2955, 2927, 2850, 1729, 1654, 1602, 1569, 1498, 1455, 1401, 1343, 1299, 1256, 1177, 1095, 1016, 968, 904, 864, 791, 725, 661 $cm^{-1}$. GPC (THF) $M_n$ 4000 g $mol^{-1}$, $M_w$ 12000 g $mol^{-1}$, PDI = 3.2.

### 2.4 Polymer-analogous reaction

**Poly[(9,9-dihexylflourene)-*alt*-(1,4-phenylenebis(*N*,*N*-dimethylaniline)methylium)] (PFC).** $AlCl_3$ (512 mg; 3.84 mmol) and **PFK** (369 mg; 0.768 mmol based on the repeat unit) were added to 40 mL freshly distilled $CH_2Cl_2$ in a dried three-necked round-bottom flask and cooled to 0 °C. To the now deep red slurry was then added *N*,*N*-dimethylaniline (931 mg; 7.68 mmol) under vigorous stirring. After complete addition the solution was allowed to warm up to rt and stirring was continued for 72 h. The deep purple reaction mixture was quenched by pouring it out over stirred 1 N HCl/ice (200 mL) before extracting with $CH_2Cl_2$ (3 × 200 mL). The organic layer was then washed with aqueous HCl and brine. Any insolubles were removed by filtration. The organic phase was washed with DI $H_2O$, concentrated, and precipitated into a large excess of alkaline $CH_3OH$, trapping the polymer as the poly(methyl ether) and turning the solution yellow. The precipitate was collected by centrifugation at 4000 rpm for 20 min and drying *in vacuo* affording **PFC-OMe** as a yellow solid (315 mg; 60%). $^1$H NMR (400 MHz, $CDCl_3$) $\delta$ 8.18–6.35 (m, 16H), 3.03–2.66 (m, 9H), 2.17–1.38 (m, 7H), 1.17–0.82 (m, 12H), 0.81–0.37 (m, 10H). FT-IR (ATR) 3293, 3033, 2955, 2924, 2854, 2794, 1657, 1607, 1562, 1518, 1464, 1403, 1347, 1258, 1201, 1095, 1013, 949, 796, 745, 723 $cm^{-1}$.

### 2.5 Cyclic voltammetry

Cyclic voltammetry (CV) was carried out with a Autolab PGSTAT100 potentiostat in a three-electrode configuration where the working electrode was ITO-coated glass (7 mm × 50 mm × 0.7 mm, 10 Ω $sq.^{-1}$, from PG&O), the counter electrode was a platinum wire, and the pseudo-reference was an Ag wire that was calibrated against ferrocene ($Fc/Fc^+$). Polymer films of **PFK** and **PFC** were spin-coated at a concentration of ~20 mg $mL^{-1}$ from $CH_3Cl$ on pre-cleaned (soap, sonicate in DI $H_2O$ 2 × 5 min, acetone 10 min, isopropanol 10 min, dry at 110 °C 10 min) and plasma oxidized (5 min) ITO-coated glass at 500–1000 rpm with 200 rpm ramp for 1 minute. Prior to spin coating, the solutions were filtered through a Gelman GHP Acrodisc 0.45 μm membrane filter. Cyclic voltammograms were recorded at 200 mV $s^{-1}$ with 0.1 M $LiClO_4$ in either acetonitrile or propylene carbonate.

### 2.6 DFT calculations

Geometries of **PFC**, **PFC-Rad$^+$**, **PFK**, and **PFK-H$^{2+}$** were optimized using Density Functional Theory (DFT) (B3LYP/6-31G**) with GAMESS-UK[26] without any symmetry constraints. For the radical **PFC-Rad$^+$**, unrestricted B3LYP was used. Subsequently, the vertical excitation energies were calculated using time-dependent DFT (TD-DFT) (B3LYPg/6-31G**) with DALTON.[27] The lowest 15 excited states were calculated for each system.

## 3 Results and discussion

### 3.1 Spinless doping

We define spinless doping as the introduction of charges into the band structure of a conjugated polymer without redox and without the spontaneous formation of unpaired spins. Spinless doping is not simply the addition of charges, but specifically the introduction of charges in the conjugated backbone *via* closed-shell, two-electron processes. Therefore, any unpaired electrons in the band structure must form spontaneously; for example, by spin un-pairing due to internal redox.[3] We distinguish between two types of spinless doping; transient, where charges are generated *in situ* and the resulting CPI cannot be isolated[4,28,29] and permanent, where the charges are generated by stabilizing trivalent carbocations *via* addition/dehydration.

Fig. 1 is a cartoon describing the differences between traditional redox doping and spinless doping. The left column shows the band structure of a CPI as cations are introduced into the backbone, in this case by masking/unmasking the cations with methoxide/acid, as is depicted for **PFC** in Scheme 1. Under acidic conditions, when there are no nucleophiles present to trap the cations, the polymer is fully conjugated and the band gap is minimized, as is shown by the red structure in the middle column. As the concentration of nucleophiles ($OCH_3^-$)

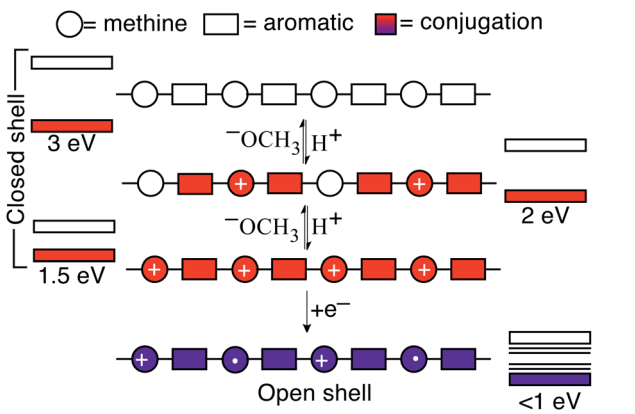


Fig. 1 A cartoon depicting the mechanism of the change in band gap of CPIs as a function of treatment with methoxide/acid compared to traditional doping. Circles indicate the methine groups that separate the aromatic groups, which are represented by squares. Conjugation is indicated in red and purple. Diagrams of the valence and conduction bands are drawn to the left or right of each structure with an approximate band gap based on Fig. 4. Increasing the concentration of nucleophiles (methoxide) traps the methine cations as $sp^3$ hybridized ethers, lowering the average conjugation length and producing a large band gap as indicated by the all-white structure. Traditional (oxidative) doping introduces both cations and unpaired spins, leading to the creation of mid-gap states and a low band-gap as indicated by the bottom, all-purple structure.

increases, the cations are trapped as $sp^3$ carbon centers (*e.g.*, methyl ethers). This process decreases the average conjugation length and increases the band gap until the polymer is rendered completely non-conjugated, represented by the white structure in the middle column. Traditional redox doping, by contrast, begins from a semiconducting polymer. The purple structure in the middle column is formed by reduction, which introduces charges *via* the addition of single electrons. This redox process also lowers the band gap, but not by affecting the average conjugation length. Rather, as is shown in the right column, it creates mid-gap states that typically lead to band gaps in the near-IR.

One of the most important differences between the CPI depicted in red and the redox-doped polymer shown in purple, is that the CPI – despite bearing charges in the band structure – can still be redox doped (by reduction). We previously observed this process *via* spectroelectrochemistry in transient CPIs.[4] In this paper, we rely on a combination of experiment and calculation to show that the same effect is present in **PFC**. However, proving that spinless doping does not induce spontaneous spin un-pairing and that CPIs are semiconductors is not straightforward. We measured the EPR spectra of both **PFK** and **PFC** and both gave no detectible signal, however, it is difficult to prove a negative. Likewise, conductivity alone is not evidence of semiconducting or metallic properties. Thus, the bulk of the Results and discussion describes the preparation and characterization of **PFK** and **PFC** and the characterization of the influences of spinless doping, which vary considerably from the well-known effects of traditional redox doping.[30]

### 3.2 Synthesis and characterization

We synthesized **PFC** *via* a Lewis acid mediated polymer analogous reaction of *N*,*N*-dimethylaniline on the cross-conjugated fluorene-based precursor polymer **PFK**. This introduction of permanent cations is spinless doping; it is an electrophilic addition/dehydration, not a redox process. We prepared **PFK** *via* the Friedel–Crafts polycondensation of fluorene **1** with terephthaloyl chloride mediated by $AlCl_3$ and LiCl in dry $CH_2Cl_2$ according to Scheme 1 and described in more detail in the Experimental. A byproduct of the Friedel–Crafts polycondensation reaction is large quantities of $AlOH_3$, which is a known flocculant and which can be challenging to separate from the desired polymer. Therefore, we attempted to minimize the $AlCl_3$ loading as much as possible and increase reaction times under highly inert conditions. We varied the Lewis acid loading for **PFK** from three to ten equivalents without negatively affecting the degree of polymerization, provided the solvents and reagents were dried and the reactions were performed under strict anhydrous conditions. Lower Lewis acid loadings resulted in a better controlled reaction and an easier isolation of **PFK**, because even with three equivalents a near-equal amount of $AlOH_3$ is formed per gram of polymer. Furthermore, we varied the polymerization time from one to three days under an Ar atmosphere. The lower Lewis acid loading and/or longer reaction times resulted in a trade-off between the degree of polymerization and polydispersity, where longer reaction times typically increase the polydispersity index (PDI) and peak molecular weight ($M_p$), but not the number average molecular weight ($M_n$).

We determined $M_n$ = 4000–5200, $M_p$ = 8000 g mol$^{-1}$, and PDI = 2.5–3.2 for **PFK** by gel permeation chromatography (GPC). See ESI† for a discussion of the batch-to-batch variability of $M_n$ and $M_p$, the effects of reaction temperature, and a comparison against model compounds. As is almost always the case, these polymers have lower values of $M_n$ than thermoplastics and block co-polymers and, thus, can be called oligomers by comparison. We prefer the term polymer because the electronic properties of conjugated polymers saturate after only a few repeats.[31,32] Thus, these materials are optically and electronically equivalent from $n \approx 5$–$\infty$ and are, therefore, more appropriately called polymers in the context of this paper. (The mechanical properties, which do vary with molecular weight, do not affect the optical or electrochemical properties.) Moreover, our estimates of $M_n$ are conservative and represent the lower bounds of the real molecular-weight distribution, rather than directly reporting the number produced by the GPC without interpretation. The most common method for determining $M_n$ (using an optical detector) relies on d$n$/d$c$ values to relate concentration to changes in the refractive index, which are then compared against a standard calibration curve. Using the common TriSEC method and d$n$/d$c$ values calculated by the instrument yielded values of $M_n$ ~24 000 g mol$^{-1}$. Since d$n$/d$c$ values are virtually unknown for conjugated polymers, they cannot be verified against published values. Furthermore, volumetric/gravimetric errors, including the material that is removed by filtration, that precipitates during the measurement, or that aggregates in solution, causes a large increase in the reported values of $M_n$. This problem is exacerbated by rigid conjugated polymers where simply measuring a GPC at elevated temperatures to reduce aggregation can change $M_n$ by an order of magnitude[33] or introduce bi-modality, which renders $M_n$ meaningless. From our conservative estimate of $M_n$ and PDI, we determined $P_n$ (the number of repeats) to be ~9–40, which is relatively low, but not atypical for a conjugated polymer. Increasing the reaction temperature (see ESI†) increased $M_p$ from 8000 to 31 000 g mol$^{-1}$, but increased the PDI.

To convert **PFK** to **PFC**, we redissolved the polymer in dry $CH_2Cl_2$ and performed a Lewis acid mediated electrophilic substitution on *N*,*N*-dimethylaniline of the activated ketones. However, when we performed the polymer analogous reaction method on **PFK** with three equivalents of $AlCl_3$ and five equivalents of *N*,*N*-dimethylaniline for one day, the conversion was low. Therefore, we repeated the polymer analogous reaction with five equivalents of $AlCl_3$ and ten equivalents of *N*,*N*-dimethylaniline for three days. Although polymer analogous reactions are never quantitative, the quality of the resulting **PFC** was unambiguously higher than the first attempt. This two-step conversion enabled us to qualitatively follow the conversion of the polymer analogous reaction spectroscopically. To render **PFC** sufficiently soluble in organic solvents, and to prevent overly strong binding of counter-ions, we isolated **PFC** as the $BF_4^-$ salt by first trapping free **PFC** with methoxide to form the non-conjugated methyl ether (*i.e.*, with $CH_3O^-$ as shown in

 

Scheme 1), dissolving it in aqueous $HBF_4$, and repeatedly extracting it with $CH_2Cl_2$.

We encountered difficulties obtaining clean $^1$H-NMR spectra of **PFC** due to problems with locking and shimming (see ESI† for examples) possibly due to the combination of the ionic and polymeric nature of CPIs driving aggregation in organic solvents (**PFC** is sparingly soluble in $CDCl_3$). Thus, we followed the process of spinless doping by FT-IR analysis, which clearly shows two carbonyl modes present in **PFK** at 1654 $cm^{-1}$ and 1725 $cm^{-1}$. Fig. 2 compares the FT-IR spectra of **PFK** to **PFC**. The intensities of these (presumed) ketone stretches decrease markedly as the ketones of **PFK** are converted to cations in **PFC**. We correlated these bands with absorption bands in the UV-Vis, allowing us to follow the process of spinless doping semi-quantitatively and, importantly, proving that the post-polymerization modification proceeds in high yield. The FT-IR spectra of model ketones and cations (single repeat-units) are shown in the ESI† to highlight the shifts that occur upon polymerization, and the very different spectra arising from the small-molecule analogs and **PFC**/**PFK**.

### 3.3 Band gap measurements

Fig. 3 and 4 show the absorption spectra of **PFK** and **PFC** respectively. The absorption spectra of **PFK** are shown in the neutral, cross-conjugated, semiconducting form and in the charged, transient spinless doped, protonated state (the solid and dashed lines in Fig. 3 respectively). Protonation shifts the band gap of **PFK** from 3.2 to 2.3 eV in a process analogous to that shown in Fig. 1 except that instead of converting between $sp^2$ methylium cations and $sp^3$ alcohols, the cations are converting cross-conjugation to linear conjugation. We measured the absorption spectra of as-prepared **PFC** and in acidified $CH_2Cl_2$ (the dashed and dotted lines in Fig. 4 respectively). By comparing the FT-IR spectra to the UV-Vis spectra, we ascribe the shoulder in the absorption spectrum of **PFC** at ~430 nm to cations resulting from the protonation of residual ketone (similar to protonated **PFK**). This peak only appears in acidified $CH_2Cl_2$, which also has the effect of red-shifting $\lambda_{max}$ by 48 nm and lowering the band gap from 1.77 to 1.55 eV. This shift is the result of maximizing the average conjugation length by converting the small amount of residual ketones from cross-conjugated carbonyls to conjugated methines and increasing the delocalization of the permanent carbocations, as is depicted

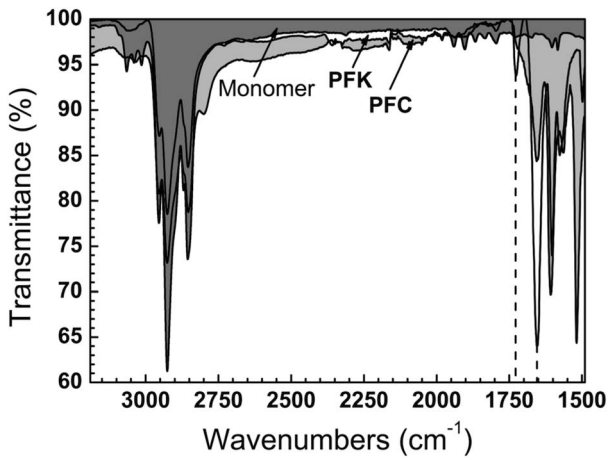


Fig. 2 FT-IR spectra showing **PFK** before (white) and after post-polymerization modification which converts it to **PFC** (light gray) by spinless doping with near completion, as indicated by the strong reduction of the carbonyl resonance mode at 1654 $cm^{-1}$ and the complete disappearance of the carbonyl mode at 1725 $cm^{-1}$, as highlighted by dashed lines.

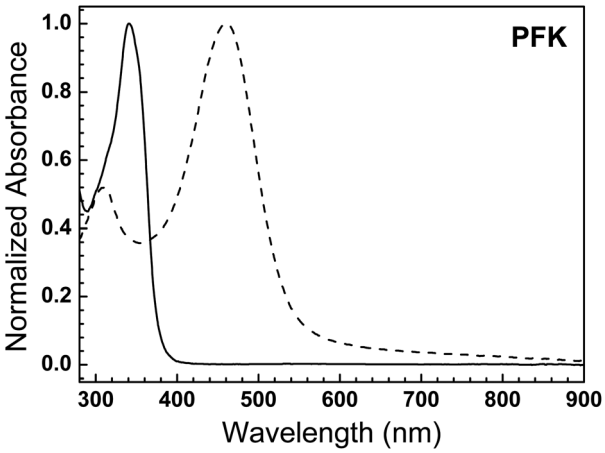


Fig. 3 Absorption spectra of **PFK** in neutral and acidified $CH_2Cl_2$ depicting a bathochromic shift of $\lambda_{max}$ by 120 nm upon transient acid doping, turning the color of the polymer from yellow to deep red. We ascribe $\lambda_{max}$ of **PFK** in neutral $CH_2Cl_2$ to weakly interacting fluorene units through cross-conjugating ketones. After the transient acid doping the polymer becomes fully conjugated resulting in the observed bathochromic shift.

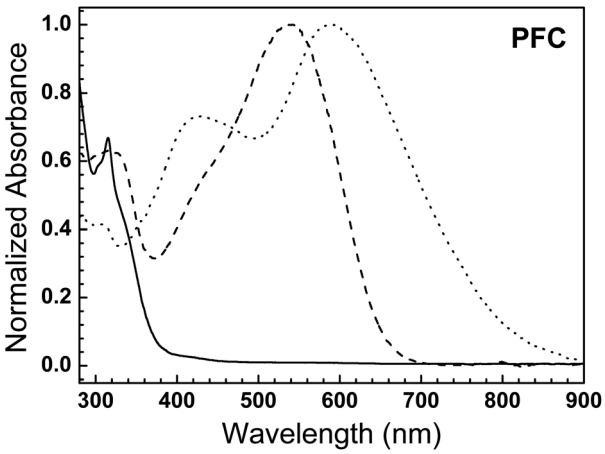


Fig. 4 Absorption spectra of **PFC** as trapped as the methyl ether **PFC-OMe** ($CH_2Cl_2$; solid line), the $BF_4^-$ salt ($CH_2Cl_2$; dashed line), and the fully protonated state (acidified $CH_2Cl_2$; dotted line). We ascribe $\lambda_{max}$ of **PFC-OMe** to the absorption of fluorene chromophores not conjugated to each other. The $BF_4^-$ salt of **PFC** has a $\lambda_{max}$ at ~540 nm and a small shoulder at ~435 nm, indicating that the residual ketones are only sparsely protonated by $HBF_4$. In acidified $CH_2Cl_2$ the residual ketones are protonated resulting in an additional bathochromic shift of ~48 nm, the appearance of an additional peak at ~430 nm, and broadening of the absorption tail (*i.e.*, lowering of the band gap).

in Fig. 1 as the all-red structure. We also measured **PFC-OMe** (the solid line in 5) by trapping **PFC** with methoxide, corresponding to the all-white structure in Fig. 1. The absorption spectrum of **PFC-OMe** cuts off at 400 nm (~3 eV) and shows no signs of residual cations (or protonated residual ketone). These absorption spectra demonstrate the dynamism of the band gap of **PFC** and its dependence on the number of conjugating cationic methines. This tunability is a unique property of CPIs that results in changes to the hybridization of carbon atoms in the backbone and should not be confused with the protonic acid doping of PANI.

To further elucidate the effect of spinless doping we measured cyclic voltammograms (CV spectra) of spin-cast films of **PFK** and **PFC** on ITO, which served as the working electrode. We used Pt wire as a counter electrode and an $Ag/Ag^+$ pseudo reference electrode calibrated with ferrocene. Measurements of **PFK** were straightforward; we cast films from $CHCl_3$ and measured them in degassed $CH_3CN$. We chose $LiClO_4$ as an electrolyte to facilitate the movement of cations in and out of the films as they were cycled. Measurements on **PFC**, by contrast, were confounded by wetting issues. **PFC** is only sparingly soluble in $CHCl_3$, giving very thin films, while thicker films cast from THF did not adhere to the electrode. Due to the ionic backbone, **PFC** is readily (and violently exothermically) soluble in acetonitrile, thus we performed the CV measurements in propylene carbonate (PC), however, $LiClO_4$ is considerably less soluble in PC. Worse, films of **PFC** tend to de-wet in PC and float off of the electrode, particularly when reduced. These experimental complexities forced us to perform CV measurements under different conditions for **PFC** and **PFK**, which can complicate direct comparison.

The results of the CV measurements are shown in Fig. 5 and 6. **PFK** shows two reduction waves at −1.7 V and −1.9 V (taken from the second scan) and a semi-reversible re-oxidation wave at ~−1.1 V with a shoulder at ~−0.8 V. We could not suppress charging effects sufficiently to resolve both re-oxidation waves clearly; neutral **PFK** is insulating enough that upon re-oxidation, charges become trapped in the film and their sudden expulsion gives rise to a small, aberrant peak (*i.e.*, retarded re-oxidation). We observed the exact same effect in previous studies on n-dopable polyketones.[4] The intensity of the redox waves appears to grow upon increasing the number of cycles suggesting retarded switching, which we ascribe to the reorganization of the polymer film as counterions diffuse into it. Larger shifts have been observed for n-type polymers,[34] but it is observed in thin films of conjugated polymers more frequently than it is reported, as the tendency is to show only one exemplary trace.

The reduction wave of **PFC** (Fig. 6), taken from the second scan, lies at −1.7 V. The entire reduction wave gradually shifts to more negative potentials and broadens to one feature upon increasing the number of scans until it stabilizes at ~−2.0 V. **PFC** re-oxidizes at a potential of ~−0.8 V. These results indicate that the cations in **PFC** are more difficult to reduce than the neutral state of **PFK**, demonstrating the remarkable stability of charges in CPIs. Not only are they delocalized into a band structure, but the electron-donating nature of the pendant dimethylaniline groups adds further stabilization. Qualitatively, the CV spectra of **PFK** show the expected two-electron reduction of cross-conjugated polyketones, while the CV spectra of **PFC** have the broad features that are typical of the reduction (or oxidation) of a band structure. If **PFC** comprised isolated cations in a "string of pearls", we would expect sharp reduction peaks.

From the optical and electrochemical data, we calculated the positions of the valence and conduction bands (*i.e.*, the bands

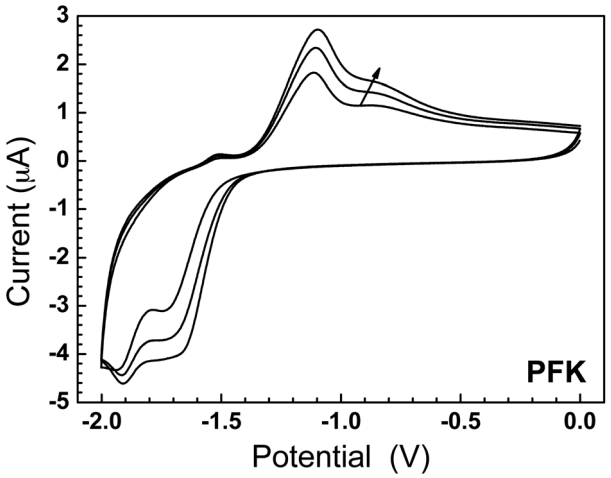


Fig. 5 Cyclic voltammograms of a thin film of **PFK** *versus* $Ag/Ag^+$ on an ITO working electrode with a Pt wire counter electrode immersed in 0.1 mM $LiClO_4$ in acetonitrile at 200 mV $s^{-1}$. The two reduction waves (−1.65 and −1.90 V) are indicative of the cross-conjugated ketones being reduced sequentially to form first a radical anion and then a closed-shell anion, *i.e.*, a transient CPI. The re-oxidation waves are partially obscured by the sudden release of trapped charge, the results from the insulator–metal–semiconductor transition, and are typical of cross-conjugated polyketones.

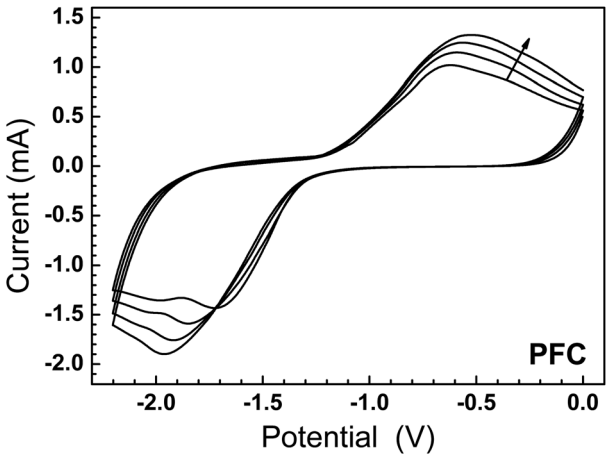


Fig. 6 Cyclic voltammograms of a thin film of **PFC** *versus* $Ag/Ag^+$ on an ITO working electrode with a Pt wire counter electrode immersed in 0.1 mM $LiClO_4$ in propylene carbonate at 200 mV $s^{-1}$. The broad, featureless reduction (~−2 V) and re-oxidation (~−0.7 V) waves are indicative of traditional redox doping/de-doping of the band structure of a semiconducting conjugated polymer. In this case, the polymer is being n-doped (reduced), to a p-doped (radical cationic) state because the semiconducting form comprises closed-shell cationic charges.

 

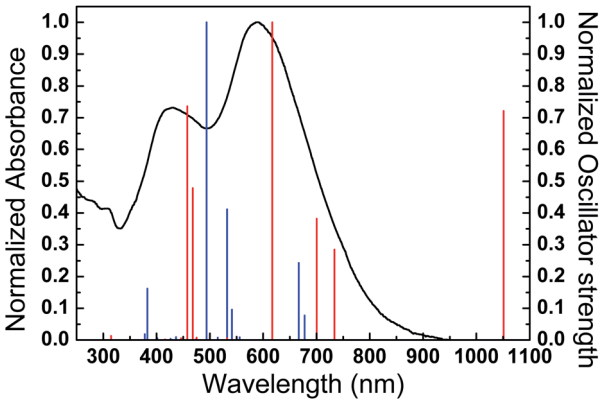


Fig. 7 The absorption spectrum of PFC (black; left axis) plotted with the predicted spectra of PFC (blue; right axis) and PFC-Rad (red; right axis). The predicted spectrum for PFC-Rad shows the emergence of a band at 1050 nm, which is in close agreement with the transient, open-shelled (redox doped) CPIs measured previously.[4]

derived from the HOMO and LUMO of the monomers, respectively) of **PFK** to be −5.83 and −2.57 eV, respectively. The values of **PFC** are −4.14 and −2.61 eV, demonstrating that spinless doping – in this case – slightly lowered the conduction band and significantly raised the valence band. This observation implies that the electron-rich dimethylaniline moieties destabilize the valence band more than the charges (which reside in the valence band) stabilize the conduction band. In other words, the dimethylaniline moieties impart more donor character than the cations impart acceptor character. The observed decrease in the band gap in **PFC** as compared to **PFK** is, therefore, principally a combination of the conversion from cross- to linear-conjugation and the destabilization of the valence band. This result is in contrast to traditional redox doping, which shifts the bands only slightly in energy and which instead lowers the band gap by creating mid-gap states that result from the presence of unpaired spins.[30]

### 3.4 DFT calculations

An ideal experiment to prove that **PFC** is an intrinsic semiconductor would be to measure the absorption spectra as a function of reduction (spectroelectrochemistry). The expectation is for the absorption band to shift from the visible into the near IR, exactly as most normal conjugated polymers behave.[4,34] Unfortunately, the poor mechanical stability of films of **PFC** at cathodic potentials precluded the collection of usable absorption data. Thus, we turned to DFT calculations for insight. The experimental design is as follows; we have absorption data for **PFK** in the neutral and protonated form, absorption data for **PFC**, and electrochemical data for **PFK** and **PFC**. From these data we calculated the optical band gaps and reduction onsets, from which we estimate the absolute positions of the valence and conduction bands. If we can replicate the optical gaps using DFT calculations, we can conclude that they behave as "normal" conjugated polymers in that their properties are predictable and that, for example, **PFC** does not undergo PISUM. We then calculate the expected optical band gap of the redox-doped state of **PFC** that is formed upon reduction, *i.e.*, we deliberately add an un-paired spin. (Interestingly, this is a case of n-doping to produce a p-doped conjugated polymer). If that band gap is significantly red-shifted, it is strong evidence that **PFC** is both spinless and is an intrinsic semiconductor because it means that our model systems are accurate reflections of the materials that we are measuring. The structures of protonated **PFK** (**PFK–H$^+$**) and the reduced form of **PFC** (**PFC-Rad**), which we measured, and the isolated model dimers **PFC**$^{2+}$, **PFC-Rad**$^+$, and **PFK-H**$^{2+}$, which we calculated, are shown in Scheme 2. The isolated model dimer of **PFK** is the deprotonated (neutral ketone) form of **PFK–H**$^{2+}$.

The calculated spectrum for **PFK** under neutral conditions comprises a minimum band gap ($E_g^{opt}$) of 3.41 eV and a main peak ($\lambda_{max}$) at 3.55 eV. These calculated peaks are blue-shifted from the experimental data by ~0.3 eV because we performed the calculations on isolated model dimers (without counter-ions), but they otherwise fit the experimental data perfectly, with the exception of an under-estimation of $E_g^{opt}$ for **PFK-H**$^+$. When protonated, $E_g^{opt}$ and $\lambda_{max}$ decrease to 2.04 eV for **PFK-H**$^{2+}$, which underestimates the experimental values likely because, experimentally, **PFK-H**$^+$ is in equilibrium and never fully protonated. These data are shown in detail in the ESI†. We calculated $E_g^{opt}$ = 1.83 eV and $\lambda_{max}$ = 2.33 eV for **PFC**$^{2+}$ as a model for **PFC** in its fully cationic state. These calculations correspond to the experimentally-derived gaps in the fully protonated state of **PFC** (in acidified $CH_2Cl_2$), *i.e.*, when all of the residual ketones are protonated and the average conjugated length of **PFC** is maximized. We calculated $E_g^{opt}$ = 1.18 eV for **PFC-Rad**$^+$ as a model for **PFC** in the redox-doped state, where one cationic site per repeat unit is replaced by a radical. That value corresponds to a maximum absorption of 1030 nm, which is well into the near IR and in close agreement with our previous transient-doping study on a related polyketone (Fig. 7).[4] The experimental and calculated data are summarized in Table 1.

The close agreement between DFT calculations and experimental values demonstrates that CPIs behave as normal,

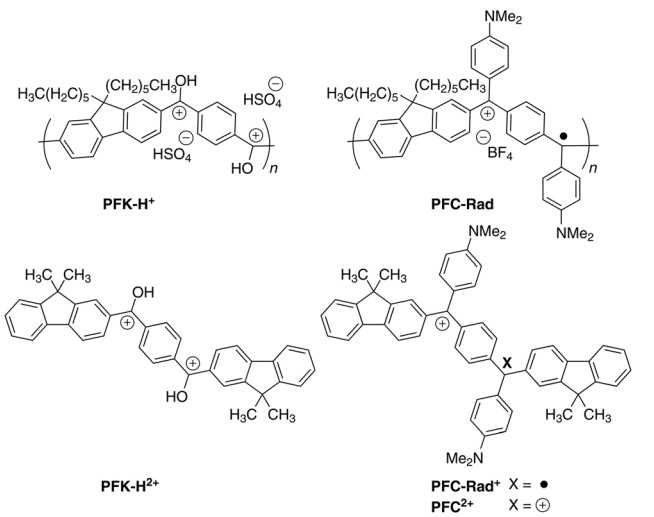


Scheme 2

Table 1 Experimental and predicted band gaps of **PFK**, **PFK-H$^+$**, **PFC**, and **PFC-Rad**; all values are in units of eV

| | $E_g^{opt}$ exp. | $E_g^{opt}$ calc. | $E_{valence}$ exp. | $E_{conduction}$ exp. |
|---|---|---|---|---|
| PFK | 3.26 | 3.41 | −5.83 | −2.57 |
| PFK-H$^+$ (PFK-H$^{2+}$) | 2.30 | 2.04 | — | — |
| PFC (PFC$^{2+}$) | 1.55 | 1.83 | −4.14 | −2.61 |
| PFC-Rad (PFC-Rad) | — | 1.18 | — | — |

intrinsic semiconducting polymers; their electronic properties are completely predictable. Thus, CPIs are in fact simply an intrinsic semiconductor polymer with charges in the valence band (*i.e.*, conjugated backbone). These data are very strong evidence that spinless doping does not lead to spontaneous spin un-pairing; if spontaneous spin un-pairing occurred, the experimental and calculated band gaps would not be in such close agreement. Moreover, the deliberate addition of unpaired electrons would not lead to a dramatic lowering of the gap.

# 4 Conclusions

The polymers presented in this paper are proofs of concept for the stabilization of closed-shell cations in the backbones of conjugated polymers. These charges are added *via* spinless doping, which chemically converts a cross-conjugated precursor polymer to a conjugated polyion; a conjugated, semiconducting polymer bearing charges in the conjugated backbone. These polymers effectively disassociate charge and spin. In traditional redox doping, polarons, which comprise both spin and charge, are created in the band structure, shrinking the band gap by creating mid-gap states. Similarly, the charges in CPIs have little effect on the absolute positions of the valence and conduction bands, which are influenced more strongly by the electron-rich groups used to stabilize the cations. However, in the absence of spin, no mid-gap states are created, thus CPIs can still undergo traditional redox doping to create (in principle) positive polarons (p-doping) through electrochemical reduction. Although we were unable to observe this phenomenon optically, DFT calculations show that, indeed, CPIs behave as normal conjugated polymers and that traditional redox doping does lead to a p-doped polymer with a significantly reduced band gap.

The key feature of CPIs is that their electronic states can be altered by chemical modification and/or redox. Unlike PANI, they are readily processible and do not undergo PISUM. A fully cationic CPI can be rendered non-conjugated by treatment with a base or nucleophile and the band gap was tuned by exposure to acid. This phenomenon is unique to CPIs and has implications for patterning, sensing, tunable absorption, and any application that takes advantage of the dynamic, post-synthetic modification of the band gap of a semiconducting polymer. The conversion of the cross-conjugated precursor polymer to the CPI *via* spinless doping also inverts the solubility by turning a hydrophobic backbone into a charged, hydrophilic backbone. In this paper that transformation rendered the CPI sparingly soluble in $CH_3Cl$ (and only as the $BF_4^-$ salt), but further manipulation of the pendant groups will allow for tunable orthogonal solubility.

Unlike virtually all light-harvesting polymers, CPIs are synthesized entirely without the use of Sn or Pd, relying on inherently scalable chemistry. (The poly[3-alkylthiophene]s and poly[alkoxy phenylene–vinylene]s are notable exceptions and, not coincidentally, have been among the most commercially successful conjugated polymers.) Yet, even **PFC** has a band gap of 1.55 eV, which can be tuned further by altering the backbone and the aryl groups used to stabilize the cations. While this paper only characterizes the influences of spinless doping, we are confident that, through the same synthetic tailoring that is commonplace in traditional conjugated polymer chemistry, CPIs will afford a variety of new conjugated materials with potential applications in organic-electronic devices.

# Acknowledgements

This work is part of the research program of the Foundation for Fundamental Research on Matter (FOM), which is part of the Netherlands Organization for Scientific Research (NWO). This is a publication by the FOM Focus Group "Next Generation Organic Photovoltaics", participating in the Dutch Institute for Fundamental Energy Research (DIFFER). The authors acknowledge the Zernike Institute for Advanced Materials of the University of Groningen for additional financial support ("Dieptestrategie" program). RCC also acknowledges the European Research Council for the ERC Starting Grant 335473 (MOLECSYNCON) and RWAH also acknowledges Prof. Dr R. Broer (University of Groningen, the Netherlands) for fruitful discussions.

# References

1 X. Guo, M. Baumgarten and K. Müllen, *Prog. Polym. Sci.*, 2013, **33**(12), 1832–1908.
2 J. Huang, S. Virji, B. H. Weiller and R. B. Kaner, *J. Am. Chem. Soc.*, 2003, **125**, 314–315.
3 F. Wudl, R. O. Angus, F. L. Lu, P. M. Allemand, D. Vachon, M. Nowak, Z. X. Liu, H. Schaffer and A. J. Heeger, *J. Am. Chem. Soc.*, 1987, **109**, 3677–3684.
4 R. C. Chiechi, G. Sonmez and F. Wudl, *Adv. Funct. Mater.*, 2005, **15**, 427–432.
5 I. Goodman, J. E. McIntryre and W. Russell, Brit. Patent, 971, 227, 1964.
6 K. J. Dahl, V. Jansons and S. Moore, Pat. No. 4,808,693, 1989.
7 J. Yang, Ph.D. thesis, Virginia Tech, 1998.
8 M. Kutz, *Applied Plastics Engineering Handbook*, William Andrew, 2011.
9 B. Azzopardi, C. J. M. Emmott, A. Urbina, F. C. Krebs, J. Mutale and J. Nelson, *Energy Environ. Sci.*, 2011, **4**, 3741.
10 H. Spanggaard and F. C. Krebs, *Sol. Energy Mater. Sol. Cells*, 2004, **83**, 125–146.
11 H. Braunling, R. Becker and G. Blochl, *Synth. Met.*, 1991, **42**, 1539–1547.

 

12 H. Braunling, G. Blochl and R. Becker, *Synth. Met.*, 1991, **41**, 487–491.
13 H. Braunling, R. Becker and G. Blochl, *Synth. Met.*, 1993, **55**, 833–838.
14 W. Chen and S. Jenekhe, *Macromolecules*, 1995, **28**, 454–464.
15 W. Chen and S. Jenekhe, *Macromolecules*, 1995, **28**, 465–480.
16 S. Jenekhe, *Nature*, 1986, **322**, 345–347.
17 N. Matsumi, K. Naka and Y. Chujo, *J. Am. Chem. Soc.*, 1998, **120**, 5112–5113.
18 N. Matsumi, K. Naka and Y. Chujo, *J. Am. Chem. Soc.*, 1998, **120**, 10776–10777.
19 R. Corriu, T. Deforth, W. Douglas, G. Guerrero and W. Siebert, *Chem. Commun.*, 1998, 963–964.
20 H. Kobayashi, N. Sato, Y. Ichikawa, M. Miyata, Y. Chujo and T. Matsuyama, *Synth. Met.*, 2003, **135**, 393–394.
21 A. Sundararaman, M. Victor, R. Varughese and F. Jäkle, *J. Am. Chem. Soc.*, 2005, **127**, 13748–13749.
22 M. Bernius, M. Inbasekaran, E. Woo, W. Wu and L. Wujkowski, *J. Mater. Sci.: Mater. Electron.*, 2000, **11**, 111–116.
23 M. Toba, T. Nakashima and T. Kawai, *Macromolecules*, 2009, **42**, 8068–8075.
24 M. Toba, T. Nakashima and T. Kawai, *J. Polym. Sci., Part A: Polym. Chem.*, 2011, **49**, 1895–1906.
25 N. Giuseppone, G. Fuks and J.-M. Lehn, *Chem. – Eur. J.*, 2006, **12**, 1723–1735.
26 M. F. Guest, I. J. Bush, H. J. J. Van Dam, P. Sherwood, J. M. H. Thomas, J. H. Van Lenthe, R. W. A. Havenith and J. Kendrick, *Mol. Phys.*, 2005, **103**, 719–747.
27 K. Aidas, C. Angeli, K. L. Bak, V. Bakken, R. Bast, L. Boman, O. Christiansen, R. Cimiraglia, S. Coriani, P. Dahle, E. K. Dalskov, U. Ekström, T. Enevoldsen, J. J. Eriksen, P. Ettenhuber, B. Fernández, L. Ferrighi, H. Fliegl, L. Frediani, K. Hald, A. Halkier, C. Hättig, H. Heiberg, T. Helgaker, A. C. Hennum, H. Hettema, E. Hjertenaes, S. Høst, I.-M. Høyvik, M. F. Iozzi, B. Jansík, H. J. A. Jensen, D. Jonsson, P. Jørgensen, J. Kauczor, S. Kirpekar, T. Kjaergaard, W. Klopper, S. Knecht, R. Kobayashi, H. Koch, J. Kongsted, A. Krapp, K. Kristensen, A. Ligabue, O. B. Lutnaes, J. I. Melo, K. V. Mikkelsen, R. H. Myhre, C. Neiss, C. B. Nielsen, P. Norman, J. Olsen, J. M. H. Olsen, A. Osted, M. J. Packer, F. Pawlowski, T. B. Pedersen, P. F. Provasi, S. Reine, Z. Rinkevicius, T. A. Ruden, K. Ruud, V. V. Rybkin, P. Sałek, C. C. M. Samson, A. S. de Merás, T. Saue, S. P. A. Sauer, B. Schimmelpfennig, K. Sneskov, A. H. Steindal, K. O. Sylvester-Hvid, P. R. Taylor, A. M. Teale, E. I. Tellgren, D. P. Tew, A. J. Thorvaldsen, L. Thøgersen, O. Vahtras, M. A. Watson, D. J. D. Wilson, M. Ziolkowski and H. Ågren, *Wiley Interdiscip. Rev.: Comput. Mol. Sci.*, 2013, DOI: 10.1002/wcms.1172.
28 K. Sugiyasu, C. Song and T. M. Swager, *Macromolecules*, 2006, **39**, 5598–5600.
29 P. A. Peart and J. D. Tovar, *J. Org. Chem.*, 2010, **75**, 5689–5696.
30 T. A. Skotheim, R. L. Elsenbaumer and J. R. Reynolds, *Handbook of Conducting Polymers*, CRC Press, New York, 2007.
31 Q. Wang, Y. Qu, H. Tian, Y. Geng and F. Wang, *Macromolecules*, 2011, **44**, 1256–1260.
32 B. Liu and S. K. Dishari, *Chem. – Eur. J.*, 2008, **14**, 7366–7375.
33 J. Li, Y. Zhao, H. S. Tan, Y. Guo, C.-A. Di, G. Yu, Y. Liu, M. Lin, S. H. Lim, Y. Zhou, H. Su and B. S. Ong, *Sci. Rep.*, 2012, **2**, 754.
34 A. K. Agrawal and S. A. Jenekhe, *Chem. Mater.*, 1996, **8**, 579–589.